

## Nonlocal optical response of weakly confined excitons in Cu<sub>2</sub>O mesoscopic films

Mitsuyoshi Takahata, Koichiro Tanaka, and Nobuko Naka\*

*Department of Physics, Kyoto University, Kitashirakawa-Oiwake-cho, Sakyo-ku, Kyoto 606-8502, Japan*

(Received 12 September 2017; revised manuscript received 8 May 2018; published 24 May 2018)

We have demonstrated size-dependent radiative coupling in a Cu<sub>2</sub>O mesoscopic film, where the spatial matching between the center-of-mass exciton motion and light waves plays an essential role. The observed quadratic increase and oscillation of the photoluminescence intensity with varying film thicknesses (16–1000 nm) indicate a nonlocal response that is unique to mesoscopic systems. Optimally, a 10<sup>4</sup>-fold enhanced radiative rate was found compared with bulk Cu<sub>2</sub>O. A new degree of freedom in the light-matter interaction is presented, which differs from the mode volume control in cavity quantum electrodynamics.

DOI: [10.1103/PhysRevB.97.205305](https://doi.org/10.1103/PhysRevB.97.205305)

### I. INTRODUCTION

The local response of an electronic system (with a dimension  $r$ ) to light (of wavelength  $\lambda$ ) is widely used when handling light-matter interactions. The local response of fundamental optical excitations, however, is not appropriate when attempting to explore coherent excited states on the *mesoscopic* scale ( $r \approx \lambda$ ). Plasmons in metal nanoparticles [1–3] and “weakly” confined excitons in wide quantum wells [4] or semiconductor thin films [5] lead to intriguing situations governed by *nonlocal* interactions [6,7]. In this instance, “weak” confinement means that the center-of-mass motion of the exciton is restricted while the relative electron-hole motion is not.

To understand the nonlocality, a microscopic description of the spatial structure beyond the long-wavelength approximation (LWA) is needed for both of the matter states and light, without macroscopic averaging. This leads to the emergence of a quantum aspect of the spatial properties, since the electronic states described by a standing wave satisfying Schrödinger’s equation are coupled with the electromagnetic waves satisfying Maxwell’s equations. In this framework, the interaction strength is expected to strongly depend on the material size because of the spatial matching condition. This size-dependent enhancement potentially exploits extremely strong coupling with light [7] and enables the selective excitation of optically forbidden states [8,9]. However, no systematic studies on the size-dependent radiative enhancement have been reported. Its observation is particularly difficult because the precise control of the material dimensions is required while maintaining the high quality to ensure a long coherence length.

In this paper, we demonstrate the size-dependent enhancement of the radiative coupling with weakly confined excitons ( $r \approx \lambda$ ), by using an artificially grown, single-crystal Cu<sub>2</sub>O thin film of continuously varying thickness for the size tuning. A unique property of the mesoscopic system was found in this study, which is in contrast to the phenomenon described within the local treatment, such as the long-range propagation

of polaritons in semiconductor slabs ( $r \gg \lambda$ ) [10,11] and the radiative enhancement of strongly confined excitons in quantum dots [12] ( $r \ll \lambda$ ) modeled by a classical dipole picture, as well as the dipole blockade of Rydberg atoms [13] utilizing the envelope wave functions.

The resonance energy shifts derived from the nonlocal response have been proved by the pioneering experiments using four-wave mixing [8,14,15] and photoluminescence (PL) [16,17] of CuCl thin films. However, direct-gap materials with large oscillator strengths, such as CuCl and GaAs, are not suitable for measurement of the radiative enhancement in the temporal domain, as recombination owing to dipole transition occurs too rapidly ( $\sim 10$  fs for the optimal enhancement). Among a variety of materials, the direct-gap semiconductor Cu<sub>2</sub>O holds an exceptional position. The conduction and valence bands of Cu<sub>2</sub>O having the same parity forbid dipole transition to the excitons with *s*-orbital relative wave function [18]. In contrast, the *p*-orbital excitons exhibit a second-class dipole transition with a small oscillator strength ( $f_{\text{Cu}_2\text{O}} = 3 \times 10^{-6} \approx f_{\text{CuCl}}/400$ ) [19], which utilizes the negative parity of the relative wave function [20]. The radiative decay of the *p*-orbital exciton is slower than the nonradiative decay even in high-quality Cu<sub>2</sub>O, such that the radiative enhancement can be observed as increased PL intensity. Therefore, Cu<sub>2</sub>O provides a unique opportunity to observe the size-dependent enhancement of the nonlocal optical response, although the weakness of the PL has so far made clear observation difficult. In the following sections, we focus first on the thickness dependence of the PL intensity and then on that of the linewidth, both of which reflect the changes in the radiative width.

### II. EXPERIMENTS

The Cu<sub>2</sub>O thin film was grown between two 0.5-mm-thick sapphire substrates [Fig. 1(a)] by the melt method [21]. The micrograph in Fig. 1(b) shows interference fringes along the  $x$  direction, indicating that the thickness of the film changes continuously in this direction, whereas it does not change in the  $y$  direction. We used our custom-built system for high-sensitivity microscopic PL measurements [22]. The sample was placed on a piezoelectric stage [Fig. 1(c)], that can be

\*naka@scphys.kyoto-u.ac.jp

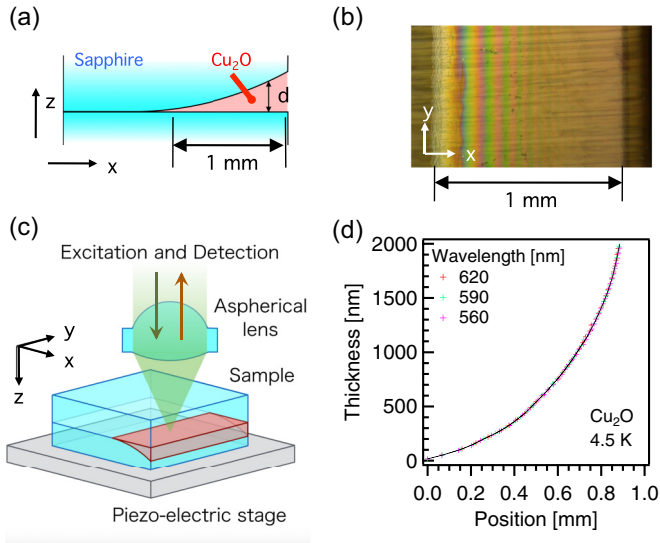


FIG. 1. (a) Schematic diagram and (b) reflection microscope image of the  $\text{Cu}_2\text{O}$  film. (c) Schematic of the PL setup. (d) Thickness of the  $\text{Cu}_2\text{O}$  film as a function of position.

moved in the  $x$ ,  $y$ , and  $z$  directions in steps of approximately 80 nm. The 532 nm continuous-wave laser light (2.0 mW) was focused on the sample using an aspherical lens (C671TME-A, Thorlabs) placed inside a cryostat. The PL from the sample was detected in a backscattering arrangement using a charge-coupled device camera at the exit of the spectrograph (CT25T, JASCO; 1200 L/mm grating). The spatial resolution was 2  $\mu\text{m}$ , which was 20-fold the diffusion length expected for  $2p$  excitons.

The transmission spectra of the film were measured at various positions. The thickness was estimated based on the interference fringes at several wavelengths [23] [Fig. 1(d)]. The thickness changed nonlinearly from 16 to 2000 nm as a function of distance because of the rounded substrate edge [see Fig. 1(a)]. Owing to the small thickness slope and the large magnification ( $\times 29$ ), a thickness resolution of 0.5–3.1 nm/ $\mu\text{m}$  was achieved for film thicknesses of 16–1000 nm. As will be discussed below, this thickness resolution is sufficiently high to observe the periodically changing radiative width in intervals of approximately 90 nm thickness.

### III. RESULTS AND DISCUSSION

Figures 2(a) and 2(b) show contour maps of the PL spectra of the  $\text{Cu}_2\text{O}$  film at 4.5 K. The solid curve on the left of Fig. 2(a) is a PL spectrum at the thickness of  $d = 471$  nm. The peaks correspond to excitons with the relative wave functions of the  $2p$ ,  $3p$ , and  $4p$  orbitals [24,25]. The solid dots in Figs. 2(c) and 2(d) show the values of the integrated PL intensity ( $I$ ) of the  $2p$  exciton peak, determined from fitting with a Lorentzian function [22]. For film thicknesses under 640 nm, the PL intensity increases in an oscillating manner in proportion to the square of the film thickness ( $I \propto d^2$ ). In contrast, for film thicknesses greater than 640 nm, the experimental data points are suppressed and vary in proportion to the film thickness while maintaining the oscillatory behavior.

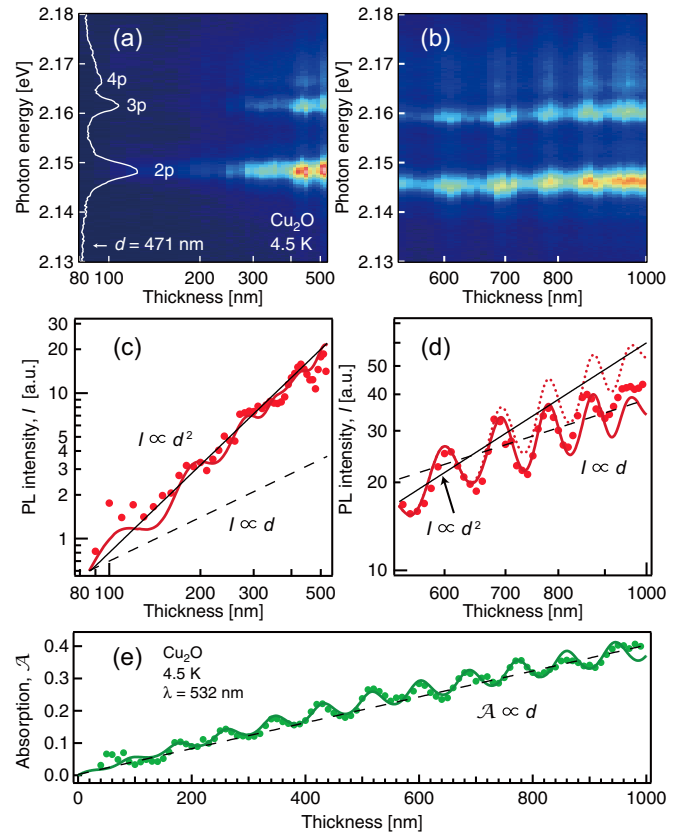


FIG. 2. (a),(b) Thickness dependence of PL spectra of the  $\text{Cu}_2\text{O}$  film at 4.5 K. The solid white line represents the PL spectrum at a thickness of 471 nm. (c),(d) PL intensity of  $2p$  excitons as a log-log plot. The solid red lines represent the calculated PL intensity by the nonlocal theory. (e) Absorption of excitation light at wavelength 532 nm. Solid line shows the calculated absorption  $\mathcal{A}$  with parameters of  $\text{Cu}_2\text{O}$  [23,26].

We consider this curious thickness dependence using a rate equation. The equation for the exciton number,  $N$ , is expressed as

$$\dot{N} = \mathcal{G} - (\gamma_r + \gamma_{nr})N, \quad (1)$$

where  $\gamma_r$  and  $\gamma_{nr}$  are the radiative and nonradiative relaxation rates, respectively. The generation rate  $\mathcal{G}$  is proportional to absorption  $\mathcal{A}$  of the excitation light.  $\mathcal{A}$  is expected to increase approximately in proportion to the film thickness because the penetration length (4  $\mu\text{m}$  [26]) of the incident laser light is much greater than the film thickness. The dots in Fig. 2(e) show the measured  $\mathcal{A}$  of the incident light, obtained by subtracting reflectance and transmittance from unity. The measured  $\mathcal{A}$  agrees with the calculation considering only multiple reflections of the incident laser light in the film between the substrates. That is,  $\mathcal{A} = 1 - |t\delta/(1 - r^2\delta^2)|^2 - |r - tr\delta^2/(1 - r^2\delta^2)|^2$ , where  $t = 4nn_s/(n + n_s)^2$ ,  $r = (n - n_s)/(n + n_s)$ , and  $\delta = \exp[-(\alpha + i2\pi n/\lambda)d]$ . Here, we used the absorption coefficient  $\alpha = 2600 \text{ cm}^{-1}$  of  $\text{Cu}_2\text{O}$  [26] and the refractive indices of  $\text{Cu}_2\text{O}$  ( $n = 3.10$ ) [23] and sapphire substrates ( $n_s = 1.77$ ).

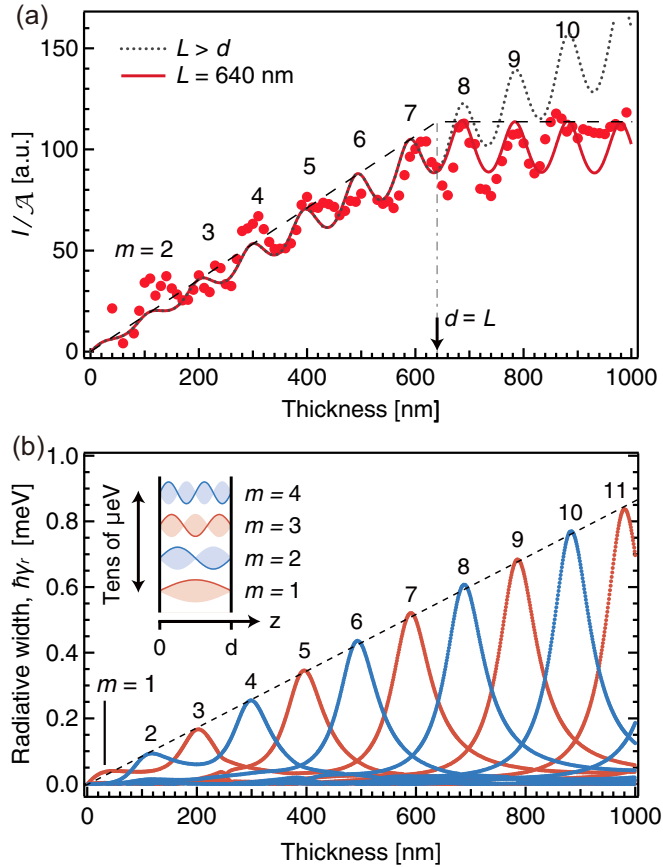


FIG. 3. (a) Thickness dependence of  $I/\mathcal{A}$  extracted from PL intensity  $I$  of the  $2p$  exciton and measured  $\mathcal{A}$  at 4.5 K (dots) in comparison with calculation results by nonlocal theory (lines). (b) Calculated radiative widths based on the nonlocal theory. The inset depicts center-of-mass wave functions of excitons labeled with their mode indices  $m$ .

By solving Eq. (1) in the steady state, the PL intensity is expressed as

$$I \propto N\gamma_r = \frac{\mathcal{G}}{\gamma_r + \gamma_{nr}} \gamma_r. \quad (2)$$

As the relation  $\gamma_{nr} \gg \gamma_r$  holds for  $\text{Cu}_2\text{O}$ , the denominator is dominated by  $\gamma_{nr}$  and hence  $I \propto (\gamma_r/\gamma_{nr})\mathcal{A}$ . Combined with the analysis of the thickness-dependent linewidth,  $\gamma_{nr}$  is found to be thickness independent (see Supplemental Material [27]). Thus the quadratic increase of the intensity can be understood by the changes not only in  $\mathcal{A}$  but also in  $\gamma_r$ .

To clarify the behavior of  $\gamma_r$  as a function of the film thickness, we plot  $I/\mathcal{A}$  for  $2p$  excitons [Fig. 3(a)].  $I/\mathcal{A}$  exhibits an increase up to a film thickness of 640 nm and the oscillatory behavior for the entire range of thicknesses investigated. The increase and oscillatory behavior suggest a nonlocal optical response, and the saturation suggests nonlocal effects with limited spatial coherence of the confined excitons.

As shown schematically in the inset of Fig. 3(b), the center-of-mass wave functions of excitons confined in a film with thickness  $d$  are indexed by the number of antinodes,  $m$ . The energy splitting of these modes is several tens of  $\mu\text{eV}$ , so they are nearly degenerate in the energy scale under

consideration. For theoretical determination of the radiative width of each mode, the Green's function approach including the nonlocal optical response is well established [7]. The polarization  $P(z, \omega)$  generated by the electric field  $E(z', \omega)$  is expressed as

$$P(z, \omega) = \epsilon_0 \int_0^d dz' \chi(z, z', \omega) E(z', \omega), \quad (3)$$

where  $\epsilon_0$  is the vacuum permittivity,  $\chi(z, z', \omega)$  is the nonlocal susceptibility, and  $\omega$  is the complex frequency. Additionally,  $E(z, \omega)$  generated by  $P(z', \omega)$  is given by

$$E(z, \omega) = \int_0^d dz' G(z, z', \omega) P(z', \omega), \quad (4)$$

where  $G(z, z', \omega)$  is the Green's function including the boundary conditions of the film [6]. Thus the self-consistent equation for the electric field is expressed as

$$E(z, \omega) = \epsilon_0 \int_0^d \int_0^d dz' dz'' G(z, z', \omega) \times \chi(z', z'', \omega) E(z'', \omega). \quad (5)$$

For given values of  $\chi(z', z'', \omega)$  and  $G(z, z', \omega)$  (see Supplemental Material [27]), we can determine  $\omega$  by finding a condition under which a nontrivial  $E(z, \omega)$  exists. Here, the integrations were performed without the LWA as assumed in Refs. [33]. The imaginary part of  $2\hbar\omega$  is the sum of the radiative width  $\hbar\gamma_r$  and the nonradiative width  $\hbar\gamma_{nr}$ . Figure 3(b) shows the calculated  $\hbar\gamma_r$  of the  $2p$  excitons, where  $\hbar\gamma_{nr} = 3.6$  meV was used. As  $\chi(z', z'', \omega)$  is a function that includes the center-of-mass wave function of mode  $m$  [34], the optical response is greatly affected by spatial matching between  $\chi(z', z'', \omega)$  and  $G(z, z', \omega)$ . Therefore, if looking at a fixed  $m$ , there is a certain value of  $d$  that maximizes  $\hbar\gamma_r$ . Upon increasing the film thickness, the mode index for the largest radiative width increases one by one.

The dotted line in Fig. 3(a) represents the calculated PL intensities obtained by summing the radiative rates over each mode, as shown in Fig. 3(b). The calculation perfectly reproduces the film thicknesses at which the local maximum or minimum appear. In addition, the modes with odd and even indices exhibited comparable enhancement following the relation  $\hbar\gamma_r \propto d$ . Within the local treatment, modes with even indices are optically forbidden [35]. Thus the comparable enhancement for neighboring modes suggests violation of the LWA.

Next, we consider the reason for the overestimation in the radiative width occurred for  $d > 640$  nm. So far, the coherence length  $L$  has been assumed to be much longer than the film thickness,  $d$ . However, in practice, the coherence length cannot be infinitely long at finite temperatures. To incorporate this effect into the calculation, we assume that the radiative width is reduced by a factor of  $L/d$  for the following reason. Numerically, we find that the radiative width increases proportionally to the film thickness [see the dashed line in Fig. 3(b)]. This can be attributed to the integral in Eq. (3),  $\int_0^d dz' = d$ . When the interaction length is limited by the coherence length, the upper limit of the integration range changes from  $d$  to  $L$ . Therefore, as an approximation, we assume that the radiative width is reduced by a factor

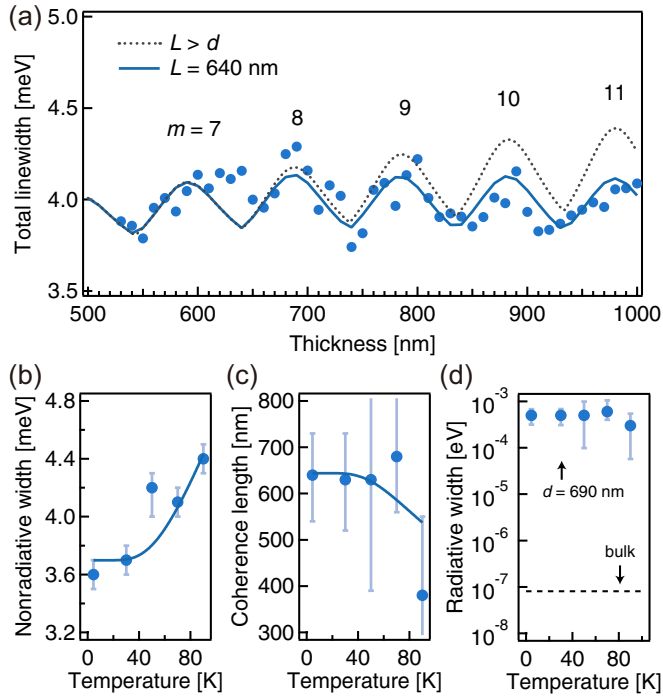


FIG. 4. (a) Thickness dependence of the total linewidth (dots) of the 2p exciton PL compared with calculations, assuming a nonlocal response with (solid line) and without (dotted line) considering the coherence length. (b)–(d) Temperature dependences of (b) nonradiative width, (c) coherence length, and (d) radiative width.

of  $L/d$  when  $L < d$ . Intuitively, saturation of the radiative width starts when the film thickness exceeds the coherence length.

The solid line in Fig. 3(a) indicates the calculation after considering the coherence length of 640 nm. The good agreement for the behavior, in terms of linear increase in  $I/A$ , oscillation, and saturation, is a clear demonstration of thickness-dependent radiative enhancement by nonlocal response and limit by the coherence length. Theoretically, if the thickness far exceeds the coherence length, the radiative enhancement is expected to decrease by the nano-to-bulk crossover [36]. The critical thickness of 9  $\mu\text{m}$  for the crossover, however, is much larger than the thickness range of the present sample.

In addition to the PL intensity, as mentioned above, the linewidth of the PL provides a direct measure of the changes in  $\hbar\gamma_r$ . The Lorentzian line shape in the PL spectra implies that the linewidth is determined by homogeneous broadening, which is the sum of  $\hbar\gamma_r$  and  $\hbar\gamma_{nr}$ . Figure 4(a) shows the thickness dependence of the total linewidth in comparison with the calculation results. Again, the experiments and calculations were found to be in excellent agreement, when the limited coherence length is considered (solid line). Comparing this result with that in Fig. 3(a), locations of enhanced PL intensity and enhanced linewidth coincide. This ensures that these changes are caused by enhancement in the radiative recombination rate rather than that in the nonradiative one.

Figures 4(b) and 4(c) show the temperature dependences of the nonradiative width and the coherence length, respectively, obtained by similar analysis. The nonradiative width increased with temperature. A coherence length of  $L \approx 600$  nm was

obtained for 4–70 K, which then decreased sharply above about 70 K. The solid line in Fig. 4(b) represents the exciton-phonon scattering rate determined by the number of phonons following the Bose distribution function [22]. The solid line in Fig. 4(c) shows the expected coherence length. This is considered to be inversely proportional to the rate of exciton-phonon scattering, which disturbs the phase of the center-of-mass motion of the excitons. It should be emphasized that the extraction of the long coherence length was made possible by the high crystalline quality of the  $\text{Cu}_2\text{O}$  film [21] and the continuously varying film thickness that well exceeded the coherence length. This coherence length corresponds to more than 100 times the Bohr radius (4 nm) of the 2p exciton, highlighting the difference in spatial extensions between the center-of-mass and relative wave functions.

Figure 4(d) shows the temperature dependence of the radiative width, which was obtained as the total linewidth minus the nonradiative width at a thickness of 690 nm. The radiative width was  $5.3 \times 10^{-4}$  eV. This value is four orders of magnitude greater than the radiative width expected for bulk  $\text{Cu}_2\text{O}$  ( $\leq 8 \times 10^{-8}$  eV; see Supplemental Material [27]). Further, it is noteworthy that our value corresponds to a high enhancement of  $10^4$ , compared with the  $10^2$ -fold enhancement measured for  $\text{CuCl}$  [16] not under the optimal matching condition.

Finally, we comment on the relation to cavity quantum electrodynamics (QED). The quality factor of the present sample is close to unity without cavity structure. Nevertheless, the radiative width of excitons in the weak confinement regime increases with the film thickness. This finding is in strong contrast to the conventional cavity QED effect. For example, spontaneous radiation by an atom in a Rydberg state is inhibited when confined in a microwave cavity with dimensions comparable with the Bohr radius [13]. The oscillator strength of strongly confined excitons in quantum wells decreases with increasing well width [37], in which not the center-of-mass but the relative motion is confined. Compared with the enhancement by the reduction of the mode volume of the photon in cavity QED, the nonlocal radiative enhancement occurs by spatial integration beyond the LWA. Thus the present result demonstrates the availability of spatial matching of the center-of-mass motion and the light wave. This concept might provide clues to overcoming the incompatibility of high radiative strength and strong antibunching in single-photon sources using Rydberg atoms [38]. The underlying physics should be extended to various systems with strong light-matter coupling, such as photonic crystals, periodic nanostructures, crystals with Mössbauer nuclei (resonant Bragg scattering) [39], and cold atoms in optical lattices [40].

#### IV. CONCLUSION

We have demonstrated the size-dependent radiative enhancement of weakly confined excitons in a  $\text{Cu}_2\text{O}$  mesoscopic film. Our experiments captured the quantum mechanical effect induced by a new degree of freedom, namely, spatial matching of the center-of-mass motion and light waves. The radiative rate was up to four orders of magnitude higher than the bulk value. The extracted coherence length ( $L = 640$  nm) was more than 100 times the Bohr radius of the 2p exciton. We believe

that the present study will trigger further interest into how the coherence length affects the luminescence properties of highly excited Rydberg states (the  $25p$  exciton) with a Bohr radius as large as  $2 \mu\text{m}$  [20] and a relative motion exceeding the light wavelength [41].

## ACKNOWLEDGMENTS

This work was partially supported by a Grant-in-Aid for Scientific Research (C) (Grant No. 26400317) and a Grant-in-Aid for Scientific Research (B) (Grant No. 17H02910) from JSPS, Japan.

- 
- [1] J. McMahon, S. Gray, and G. Schatz, Nonlocal Optical Response of Nanostructures with Arbitrary Shape, *Phys. Rev. Lett.* **103**, 097403 (2009).
- [2] N. Mortensen, S. Raza, M. Wubs, T. Søndergaard, and S. Bozhevolnyi, A generalized non-local optical response theory for plasmonic nanostructures, *Nat. Commun.* **5**, 3809 (2014).
- [3] H. Shen, L. Chen, L. Ferrari, M. Lin, N. Mortensen, S. Gwo, and Z. Liu, Optical observation of plasmonic nonlocal effects in 2D superlattice of ultrasmall gold nanoparticles, *Nano Lett.* **17**, 2234 (2017).
- [4] E. S. Khrantsov, P. A. Belov, P. S. Grigoryev, I. V. Ignatiev, S. Yu. Verbin, Yu. P. Efimov, S. A. Eliseev, V. A. Lovtcius, V. V. Petrov, and S. L. Yakovlev, Radiative decay rate of excitons in square quantum wells: Microscopic modeling and experiment, *J. Appl. Phys.* **119**, 184301 (2016).
- [5] H. Ishihara, K. Cho, K. Akiyama, N. Tomita, Y. Nomura, and T. Isu, Large Four-wave Mixing of Spatially Extended Excitonic States in Thin GaAs Layers, *Phys. Rev. Lett.* **89**, 017402 (2002).
- [6] K. Cho, *Optical Response of Nanostructures: Microscopic Non-local Theory* (Springer, New York, 2003).
- [7] H. Ishihara, J. Kishimoto, and K. Sugihara, Anomalous mode structure of a radiation-exciton coupled system beyond the long-wavelength approximation regime, *J. Lumin.* **108**, 343 (2004).
- [8] M. Ichimiya, M. Ashida, H. Yasuda, H. Ishihara, and T. Itoh, Observation of Superradiance by Nonlocal Wave Coupling of Light and Excitons in CuCl Thin Films, *Phys. Rev. Lett.* **103**, 257401 (2009).
- [9] T. Iida and H. Ishihara, Unconventional control of excited states of a dimer molecule by a localized light field between metal nanostructures, *Phys. Status Solidi A* **206**, 980 (2009).
- [10] D. Fröhlich, A. Kulik, B. Uebbing, V. Langer, H. Stolz, and W. Ostern, Propagation Beats of Quadrupole Polaritons in  $\text{Cu}_2\text{O}$ , *Phys. Rev. Lett.* **67**, 2343 (1991).
- [11] G. Malpuech, A. Kavokin, and G. Panzarini, Propagation of exciton polaritons in inhomogeneous semiconductor films, *Phys. Rev. B* **60**, 16788 (1999).
- [12] T. Itoh, M. Furumiya, T. Ikehara, and C. Gourdon, Size-dependent radiative decay time of confined excitons in CuCl microcrystals, *Solid State Commun.* **73**, 271 (1990).
- [13] R. G. Hulet, E. S. Hilfer, and D. Kleppner, Inhibited Spontaneous Emission by a Rydberg Atom, *Phys. Rev. Lett.* **55**, 2137 (1985).
- [14] M. Ichimiya, K. Mochizuki, M. Ashida, H. Yasuda, H. Ishihara, and T. Itoh, Efficient radiative recombination of multinode-type excitons up to room temperature in CuCl thin films, *J. Lumin.* **131**, 498 (2011).
- [15] M. Ichimiya, H. Yasuda, M. Ashida, H. Ishihara, and T. Itoh, Room temperature superradiance due to coherent coupling between light and extended single quantum state, *J. Non-Cryst. Solids* **358**, 2357 (2012).
- [16] L. Q. Phuong, M. Ichimiya, H. Ishihara, and M. Ashida, Multiple light-coupling modes of confined excitons observable in photoluminescence spectra of high-quality CuCl thin films, *Phys. Rev. B* **86**, 235449 (2012).
- [17] T. Matsuda, N. Yokoshi, and H. Ishihara, Upconverted photoluminescence induced by radiative coupling between excitons, *Phys. Rev. B* **93**, 155418 (2016).
- [18] H. Matsumoto, K. Saito, M. Hasuo, S. Kono, and N. Nagasawa, Revived interest on yellow-exciton series in  $\text{Cu}_2\text{O}$ : An experimental aspect, *Solid State Commun.* **97**, 125 (1996).
- [19] J. B. Grun and S. Nikitine, Etude de la forme des raies des series jaune et verte de la cuprite, *J. Phys.* **24**, 355 (1963).
- [20] T. Kazimierzczuk, D. Fröhlich, S. Scheel, H. Stolz and M. Bayer, Giant Rydberg excitons in the copper oxide  $\text{Cu}_2\text{O}$ , *Nature (London)* **514**, 343 (2014).
- [21] N. Naka, S. Hashimoto, and T. Ishihara, Thin films of single-crystal cuprous oxide grown from the melt, *Jpn. J. Appl. Phys.* **44**, 5096 (2005).
- [22] T. Kitamura, M. Takahata, and N. Naka, Quantum number dependence of the photoluminescence broadening of excitonic Rydberg states in cuprous oxide, *J. Lumin.* **192**, 808 (2017).
- [23] A. E. Rakhshani, Measurement of dispersion in electrodeposited  $\text{Cu}_2\text{O}$ , *J. Appl. Phys.* **62**, 1528 (1987).
- [24] K. Reimann and K. Syassen, Raman scattering and photoluminescence in  $\text{Cu}_2\text{O}$  under hydrostatic pressure, *Phys. Rev. B* **39**, 11113 (1989).
- [25] The deviation of the resonance energy around the film thickness of 520 nm is probably due to strain.
- [26] C. Malerba, F. Biccari, C. Ricardo, M. D’Incau, P. Scardi, and A. Mittiga, Absorption coefficient of bulk and thin film  $\text{Cu}_2\text{O}$ , *Sol. Energy Mat. Sol. Cells* **95**, 2848 (2011).
- [27] See Supplemental Material at <http://link.aps.org/supplemental/10.1103/PhysRevB.97.205305> for details of the nonlocal optical theory and estimation of radiative and nonradiative widths, which includes Refs. [28–32].
- [28] N. Naka, I. Akimoto, M. Shirai, and K. Kan’no, Time-resolved cyclotron resonance in cuprous oxide, *Phys. Rev. B* **85**, 035209 (2012).
- [29] S. Zielińska-Raczyńska, D. Ziemkiewicz, and G. Czajkowski, Electro-optical properties of Rydberg excitons, *Phys. Rev. B* **94**, 045205 (2016).
- [30] D. W. Snoko, A. J. Shields, and M. Cardona, Phonon-absorption recombination luminescence of room-temperature excitons in  $\text{Cu}_2\text{O}$ , *Phys. Rev. B* **45**, 11693 (1992).
- [31] H. Stolz, F. Schöne, and D. Semkat, Interaction of Rydberg excitons in cuprous oxide with phonons and photons: Optical linewidth and polariton effect, *New J. Phys.* **20**, 023019 (2018).
- [32] G. Hoof, W. Poel, and L. Molenkamp, Giant oscillator strength of free excitons in GaAs, *Phys. Rev. B* **35**, 8281 (1987).
- [33] E. L. Ivchenko, Excitonic polaritons in periodic quantum-well structures, *Sov. Phys. Solid State* **33**, 1344 (1991).

- [34] S. I. Pekar, The theory of electromagnetic waves in a crystal in which excitons are produced, *Zh. Eksp. Teor. Fiz.* **33**, 1022 (1958) [*Sov. Phys. JETP* **6**, 785 (1958)].
- [35] Z. K. Tang, A. Yanase, T. Yasui, Y. Segawa, and K. Cho, Optical Selection Rule and Oscillator Strength of Confined Exciton System in CuCl Thin Films, *Phys. Rev. Lett.* **71**, 1431 (1993).
- [36] M. Bamba and H. Ishihara, Crossover of exciton-photon coupled modes in a finite system, *Phys. Rev. B* **80**, 125319 (2009).
- [37] Y. Masumoto, M. Matsuura, S. Tarucha, and H. Okamoto, Direct experimental observation of two-dimensional shrinkage of the exciton wave function in quantum wells, *Phys. Rev. B* **32**, 4275(R) (1985).
- [38] M. Saffman, T. G. Walker, and K. Molmer, Quantum information with Rydberg atoms, *Rev. Mod. Phys.* **82**, 2313 (2010).
- [39] U. van Bürck, R. L. Mössbauer, E. Gerdau, R. Ruffer, R. Hollatz, G. V. Smirnov, and J. P. Hannon, Nuclear Bragg Scattering of Synchrotron Radiation with Strong Speedup of Coherent Decay, Measured on Antiferromagnetic FeBO<sub>3</sub>, *Phys. Rev. Lett.* **59**, 355 (1987).
- [40] M. Weidemüller, A. Hemmerich, A. Görlitz, T. Esslinger, and T. W. Hänsch, Bragg Diffraction in an Atomic Lattice Bound by Light, *Phys. Rev. Lett.* **75**, 4583 (1995).
- [41] S. Zielińska-Raczyńska, G. Czajkowski, and D. Ziemkiewicz, Optical properties of Rydberg excitons and polaritons, *Phys. Rev. B* **93**, 075206 (2016).